

The failure of the Tacoma Bridge: A physical model

Daniel Green and William G. Unruh

Citation: *Am. J. Phys.* **74**, 706 (2006); doi: 10.1119/1.2201854

View online: <http://dx.doi.org/10.1119/1.2201854>

View Table of Contents: <http://ajp.aapt.org/resource/1/AJPIAS/v74/i8>

Published by the [American Association of Physics Teachers](#)

Related Articles

The Enigma of the Aerofoil: Rival Theories in Aerodynamics, 1909–1930.

Am. J. Phys. **80**, 649 (2012)

Simple, simpler, simplest: Spontaneous pattern formation in a commonplace system

Am. J. Phys. **80**, 578 (2012)

Determination of contact angle from the maximum height of enlarged drops on solid surfaces

Am. J. Phys. **80**, 284 (2012)

Aerodynamics in the classroom and at the ball park

Am. J. Phys. **80**, 289 (2012)

The added mass of a spherical projectile

Am. J. Phys. **79**, 1202 (2011)

Additional information on Am. J. Phys.

Journal Homepage: <http://ajp.aapt.org/>

Journal Information: http://ajp.aapt.org/about/about_the_journal

Top downloads: http://ajp.aapt.org/most_downloaded

Information for Authors: <http://ajp.dickinson.edu/Contributors/contGenInfo.html>

ADVERTISEMENT



WebAssign[®]

The **PREFERRED** Online Homework Solution for Physics

Every textbook publisher agrees! Whichever physics text you're using, we have the proven online homework solution you need. WebAssign supports every major physics textbook from every major publisher.

webassign.net

CENGAGE Learning WILEY
openstax COLLEGE W.H. FREEMAN
Physics Curriculum & Instruction
McGraw Hill Higher Education PEARSON

The failure of the Tacoma Bridge: A physical model

Daniel Green^{a)} and William G. Unruh^{b)}

Department of Physics and Astronomy, University of British Columbia, Vancouver, BC V6T 1Z1, Canada

(Received 23 August 2004; accepted 7 April 2006)

The cause of the collapse of the Tacoma Narrows Bridge has been a topic of much debate and confusion over the years. Many mischaracterizations of the observed phenomena have limited the understanding of the collapse even though there has always been an abundance of evidence in favor of a negative damping model. Negative damping, or positive feedback, is responsible for large amplitude oscillations in many systems, from musical instruments to the Tacoma Narrows Bridge failure. We discuss some of the more well known examples of positive feedback, and then show how the interaction of the wind with the oscillating bridge, especially the development of large scale vortices above and below the deck of the bridge, led to such a positive feedback instability. We support our model by computational, experimental, and historical data. © 2006 American Association of Physics Teachers.

[DOI: 10.1119/1.2201854]

I. INTRODUCTION

One of the most surprising of physical phenomena is the conversion of a steady state condition into oscillations. Examples include the steady blowing of air through the reed of a clarinet, the flow of air over the blow hole of a flute or over the neck of a beer bottle, and the conversion of the steady pull of a bow across a string in a violin into a steady vibration.¹ In some of these examples the mechanism is clear and direct, and in others it depends on a time delayed feedback mechanism to produce the instability associated with the sound production. The howl of a sound amplification system if the microphone is too near the speakers is the most common example of such a phenomenon. The reed instruments and the violin bow operate under conditions in which they act as sources of negative damping in which the instability converts arbitrarily small input signals into larger outputs.

If the external pressure on a clarinet reed is high enough to partially close the reed (but not so high as to completely close it), an increase in the internal pressure will open the reed and allow more air into the clarinet. A decrease in internal pressure will close the reed and allow in less air. That is, more air enters the instrument when the pressure is high and less enters when the pressure is low. Energy is fed into the system as a result. The negative slope in the pressure flow rate curve results in negative damping for oscillations within the instrument, causing the amplitude to increase until the reed enters a highly nonlinear regime.

Similarly, for the violin bow the presence of the rosin on the bow creates a negative damping regime in which the force on the string decreases as the relative velocity between the string and the bow increases. This effect will amplify any oscillations in the string. Because the effect is greatest on the resonant modes of the string, the negative damping regime tends (if the bow is properly played) to create large amplitude oscillations at the resonant frequency of the string. The oscillation increases in amplitude until the nonlinear stick-slip amplitude is reached.

For the flute or the coke bottle the effect is more subtle and involves a time delay. The player blows a steady stream of air across the hole such that if the air in the bottle did not oscillate, the stream would hit the far side of the hole and be diverted, half into and half out of the flute or bottle. But, if

the air inside the instrument is vibrating, there will be an in-out airflow of the hole caused by the vibration. This vibration deflects the stream directed across the bottle. While the deflection is maximum at the point of maximum flow of air into or out of the instrument, it takes a finite time for the stream to cross the opening and either enter or exit the instrument. If this time delay is a quarter of a period, then the stream will be deflected into the instrument when the pressure within is highest, and will be deflected out when the pressure inside is lowest. Just as for the clarinet, the stream does work on the air inside the instrument, leading to an instability and sound production. There is no direct source of the amplification. Rather it is an interaction between the oscillations of the air in the instrument and the airflow across the opening (see Fig. 1). Only those modes with the correct relation between the oscillation period and the time it takes the air to flow across the hole are amplified, and thus have a negative damping coefficient. In this case it is the timing of the airflow across the opening that is crucial for establishing the instability which creates the large oscillation.

There are two important aspects in all of these examples. Although the natural oscillation period of the vibration produced tends to be very close to the period of a natural resonance of the instrument (the air within the tube of a clarinet, flute or beer bottle, and the string of a violin) none of these correspond to the traditional notion of resonance. There is no external oscillating force that is tuned to the natural period of the oscillation. Rather there is a complex nonlinear interaction between the oscillations and the external steady action which creates a condition of negative damping and instability for the natural modes of oscillation of the instrument.

That it is the natural modes that are important can be seen by looking at the equation of motion for the oscillator.

$$M \frac{d^2x}{dt^2} + Kx + 2M\gamma \frac{dx}{dt} = 0. \quad (1)$$

If γ is negative, the solutions are oscillatory with a frequency very near the natural frequency $\sqrt{K/M}$, but with an exponentially growing amplitude. There is nothing about γ that needs to have anything to do with that natural period. That is, the only role that the external conditions (pressure on the clarinet reed, motion of the bow, air stream blowing across the beer

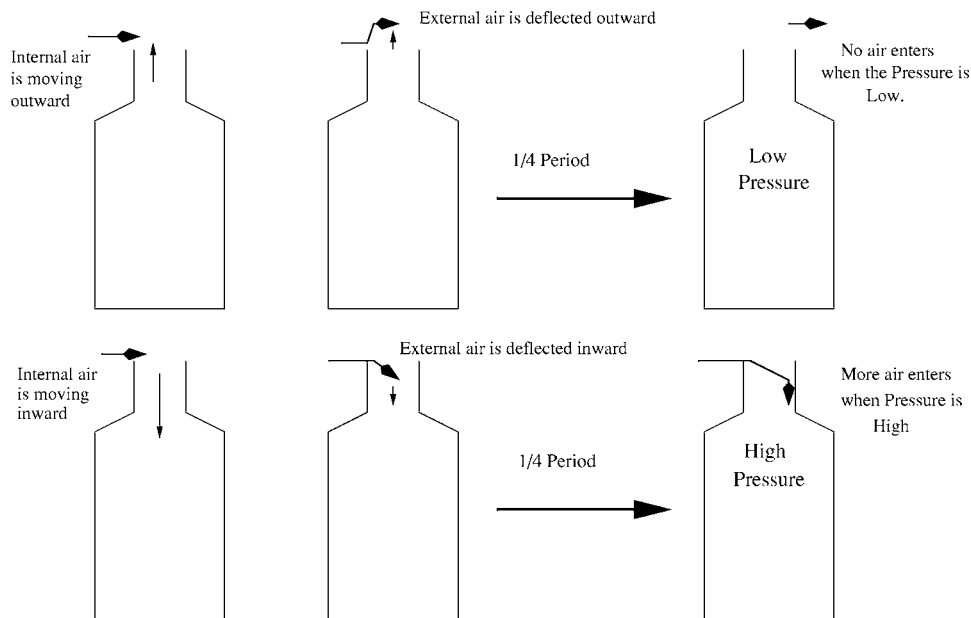


Fig. 1. The positive feedback that occurs between the internal oscillations of a bottle and external air blown over the surface at $1/4$ the period of the internal oscillations. The result is an exponentially increasing oscillation that we can hear.

bottle) need play is to set up the conditions needed to make γ negative.

One of the most impressive examples of a conversion of a more or less steady flow of air into a large amplitude vibration was that of the Tacoma Narrows Bridge. As Billah and Scanlan complained 13 years ago,² physics textbooks have called this large scale oscillation an example of a resonance, when it was clearly not. Already in the report by Ammann, von Karmen, and Woodruff³ to the Federal Works Agency that investigated the collapse (a report issued only four months after the collapse), it was recognized that the collapse was due to an example of negative damping, just as in the musical instruments we have mentioned. This conclusion was based on wind tunnel experiments carried out at the California Institute of Technology, which clearly showed the exponential growth of the oscillations. Physicists have ignored or been ignorant of this report, perhaps in part because it left the physical origin of this negative damping unclear.

What is that physical origin? It must be some aspect of the turbulence in the flow of the wind across the bridge, but which aspect? This paper will discuss recent work that attempts to clarify the origin of the feedback, which resulted in such an impressive example of a natural “musical instrument.”

The Tacoma Narrows Bridge opened on July 1, 1940 and collapsed on November 7, 1940 under winds of approximately 40 mph. During this brief period of existence, the bridge became an attraction as it oscillated at a relatively low amplitude (a few feet at the very most) in a number of different modes, in all of which the bridge deck remained horizontal. Low mechanical damping allowed the bridge to vibrate for long periods of time. However, on November 7 at 10:00 a.m., torsional oscillations began that were far more violent than anything seen previously. (The oscillations were measured at one time to have an amplitude of $\approx 13'$, or because the width of the bridge was about $39'$, greater than 0.7 rad.) At 11:10 am, the mid-span of the deck broke and fell due to the large stresses induced by the oscillation. The

H-shape of the bridge cross section, together with its slender design, were recognized as crucial components of the problem. The post-facto study of the instability of such bridge sections in wind tunnel tests, which formed the core of the Ammann *et al.* report,³ resulted in the realization by the engineering community that dynamical studies, such as those that had been carried out by the report’s authors, were crucial before building future bridges. The calculation of static wind forces, which the bridge had to be more than capable of withstanding, was not sufficient. That the importance of such dynamical studies has not yet been absorbed by the engineering community is evidenced by the public forced closure of the Millennium footbridge in London in 2000, one day after opening, due to a similar feedback instability, this time between the bridge and the reaction times of people walking across it.⁴

At this point, we might ask, “This collapse happened so long ago, bridges today are stable, why do we care?” Although it is possible to find stable bridges by trial and error, a physical understanding would be valuable. For these reasons, we would like to understand the nature of the feedback that caused the failure. In this paper we will examine a physical model for the collapse of Tacoma Narrows Bridge. First we will revisit old explanations that gloss over the underlying problem. Our model will then be presented, followed by supporting evidence from historical, computational, and experimental data.

II. HISTORICAL MISCONCEPTIONS

The underlying cause of the collapse of the Tacoma Narrows Bridge has been frequently mischaracterized. Although evidence in favor of negative damping has been available since 1941,³ oversimplified and limited theories have dominated popular literature and undergraduate physics textbooks. Billah and Scanlan² have described and analyzed many of the frequently quoted explanations. Most commonly, the collapse is described as a simple case of reso-

nance. There exists a video (the attribution on our copy has been lost so we cannot reference the authors) in which the instability is modeled by a fan blowing on a set of thick horizontal rods fastened to a central perpendicular wire around which the rods oscillate. The demonstrator inserts and removes a large piece of cardboard in front of the fan at the resonant frequency of the rods and states that this type of fluctuation in the wind blowing on the bridge is how the bridge was excited into its violent oscillation. However, this comparison to a forced harmonic oscillator requires that the wind generate a periodic force tuned to the natural frequency of the bridge. The video remarks that “texts are vague about what the exciting force was and just how... it acquired the necessary periodicity.”

As discussed by Billah and Scanlan,² in some explanations the periodic vortex shedding of the bridge was the source of this periodicity (the von Karman vortex street).⁵ Such models assume that the frequency of vortex shedding (the Strouhal frequency) matches the natural frequency of the bridge. However, the Strouhal frequency of the bridge under a 42 mph wind is known to be about 1 Hz, far from the observed 0.2 Hz natural frequency of the bridge. The von Karman vortex street could not produce resonant behavior on the day of the collapse. This mismatch in frequencies between the van Karman vortex shedding and the bridge frequency is also clear in our computer modeling of the airflow over the bridge that we will discuss. Furthermore, to create such a huge response in the bridge, its Q value must have been absurdly high, with the concomitant requirement that the frequency of the wind gusts be accurately tuned to that resonant frequency to an accuracy of $1/Q$.

Although Billah and Scanlan² clearly outline the pitfalls of the resonance model, recent work⁶ has attempted to resurrect this model with a nonlinear oscillator. For a nonlinear oscillator, the frequency can change as the amplitude changes. This dependence can lead to complex and even chaotic behavior of the oscillator. Let us look at the solution of the nonlinear equation

$$\frac{d^2y}{dt^2} + \beta \frac{dy}{dt} + \tanh y = F \sin \Omega t. \quad (2)$$

Equation (2) represents a simple model in which the restoring force ($\tanh y$) goes from linear dependence at small amplitude y to a constant restoring force for large y . In Fig. 2 we plot the long-term amplitude of the oscillation of the system as a function of the frequency Ω and the magnitude F of the external sinusoidal force. In general, the long-term behavior of $y(t)$ is an approximately harmonic solution in t . (For Ω very different from the resonance value of unity for small oscillations and F near unity, we can also obtain highly nonharmonic chaotic behavior even at late times, but we will not discuss this behavior here.) There is a discontinuity in the amplitude of the long-term solution of Eq. (2) as a function of F for Ω less than the small amplitude resonance frequency of unity. As $\Omega \rightarrow 1$, the discontinuity disappears. In all cases the initial values of y and dy/dt are zero. Other solutions not displayed in Fig. 2 show that the location of the discontinuity (value of F for a given Ω where the discontinuity in the amplitude appears) can depend on these initial values.

This discontinuous behavior eliminates one of the problems with the standard physics textbook explanation of the bridge motion by resonance, namely that the wind speed would have to be absurdly accurately tuned so that the reso-

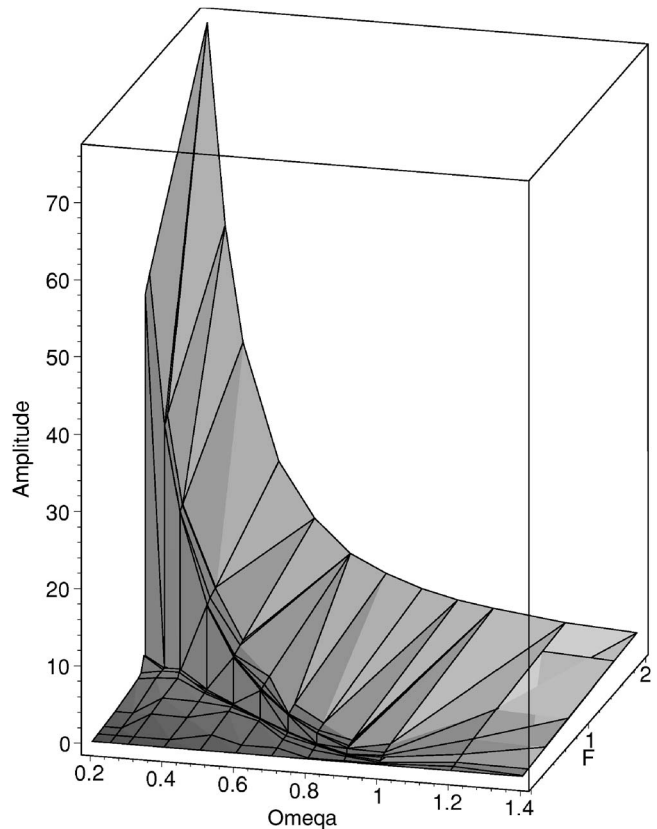


Fig. 2. A contour plot of the long-term amplitude of a driven oscillator with a $\tanh(y)$ restoring force as a function of the frequency Ω and amplitude F of the external sinusoidal force. Note the sharp discontinuity as a function of F for $\Omega < 1$, the small amplitude free oscillation frequency.

nance condition would produce the incredibly high amplitudes of oscillation. Once the driving amplitude was large enough that the bridge entered the upper part of the resonance curve, the bridge’s motion could remain at large amplitudes even as the frequency of the driving force is varied. It is these features of the nonlinear model, namely the tracking of the frequency of the external force, and the potential for sudden discontinuities in the amplitude of the motion that McKenna *et al.*⁷ see as the key advantage of this model.

This model could also explain a puzzling anomaly in the bridge’s motion on November 7. At about 6 a. m. on November 7 the bridge began to oscillate in a nontorsional mode, with a relatively low amplitude ($\approx 1.5'$), and about 8 or 9 nodes in the oscillation along the length of the bridge. Suddenly at around 10 a. m., while Kenneth Arkin, Chairman of the Washington Toll Bridge Authority, was trying to measure the amplitude of oscillations with a surveyor’s transit,

“... the mid span targets disappeared to the right of my vision. Looking over the transit, mid span seemed to have blown north approximately half the roadway width coming back into position in a spiral motion....”³

That is, the transition to the very large amplitude torsional oscillation was very abrupt. The bridge went from no torsional oscillation to a very large torsional oscillation almost instantaneously. This change seemed to occur with little

change in the wind velocity (the often quoted 42 mph for the wind was measured on the deck of the bridge before the bridge went into its torsional oscillation). The report's conclusion was that this transition was occasioned by the sudden slipping of a retaining collar on the main suspension cable.

McKenna and co-workers⁷ have used this description to argue that what happened at that moment was that the bridge suddenly made a transition from the lower amplitude solution to the upper, perhaps due to the effect of a gust of wind. In their model for the bridge they introduce the nonlinearity by describing the effect of the cables on the bridge as "one-sided springs" rather than as Hooke's law type springs. Thus, when the side of the bridge rose above its normal equilibrium position, the cables on that side were assumed to go slack, putting the bridge into free fall [with gravity the only restoring force; the tanh dependence in the force function in Eq. (2) mimics this behavior]. As is well known from watching a bouncing ball, when gravity is the only restoring for an object, the frequency of oscillation decreases as the amplitude increases, just as in Eq. (2). If the cables on the bridge went slack during the oscillation of the bridge, its behavior is comparable to the bouncing ball. However, there is no indication in any of the reports of the engineers watching the oscillation that the supports slackened. In fact, Farquarson, one of the chief consultants, went onto the bridge during its violent torsional oscillation to observe the behavior of the bridge and in a failed attempt to rescue a car and dog abandoned on the bridge. He reported that the riser cables were not slack during the oscillation.³

In addition to his original suggestion, McKenna⁷ suggested that perhaps the use of the appropriate trigonometric functions instead of the linear approximation could provide sufficient nonlinearity. From their numerical calculations of the response of such a nonlinear oscillator, given by

$$\frac{d^2\theta}{dt^2} + \sin(\theta) = F \sin(\omega t), \quad (3)$$

with a force with constant frequency ω and amplitude F , they argued that the nonlinearities of the trigonometric functions *alone* can give the same kind of bimodal response with large amplitude oscillations. However, this jump in amplitude for the $\sin(\theta)$ potential would be similar to Eq. (2) near $\Omega=1$ where the jump in the amplitude of the oscillation is not very large.

Although Refs. 6 and 7 provide a more complete description of the observed motion, they ignore the cause of the driving forces. In particular, these models assume that there exists an external sinusoidal force on the bridge with constant period and amplitude (chosen for their ability to drive the resonance) without regard for their physical origin. However, even if such a bimodal nonlinear response is similar to the actual response of the bridge to external forces, little insight into the cause of the collapse is gained without understanding the origin of these forces.

These nonlinear oscillator models do not address the wealth of data collected in wind tunnels and on the day of collapse. In particular, the logarithmic decrement of the oscillation (effective negative damping coefficient) had already been measured over an extensive range of wind speed in wind tunnel tests immediately after the collapse.³ These results reveal that the wind induced damping coefficient changes from positive to negative at a critical wind speed. Above this critical wind speed, the behavior of the negative



Fig. 3. Frame from the film taken by Elliot *et al.* (Ref. 8) of the bridge collapse. In the frame the wind moves from left to right. To the right of the car is a large vortex outlined by the cement dust from a section of the roadway that was apparently disintegrating. On the left sits Professor Farquarson. This frame is a blowup of a small section of the 8 mm film. Due to the eye's motion tracking ability, the behavior of the vortex is much clearer in the film. The roadway is almost level in its counterclockwise rotation and the low pressure vortex is thus feeding energy into the bridge motion. Copyright by The Camera Shop. Used with permission.

damping coefficient appears to be linear in the wind velocity. It should be possible to explain these and other results with a realistic model. Most important, we should be able to describe what specific features of the Tacoma Narrows Bridge caused it to collapse. Because nonlinearities are present in all suspension bridges, why do other bridges remain stable even in high winds? Although nonlinear models may provide some insight into the motion of large span bridges, they do not address these questions.

III. VORTICES AGAIN?

An important clue to the bridge collapse is given in a few frames of the films taken by Elliot.⁸ At one point the concrete in the bridge deck begins to break up and throws dust into the air. This dust acts as a tracer for the airflow over the bridge. In Fig. 3 we can just see a large vortex moving across the bridge beyond and to the right of the car abandoned on the bridge (the development in the movie is much clearer). The vortex is first observed at just about the point where the oscillation of the bridge is at a point where the roadway is level and the windward edge of the bridge is rising; by the time the bridge reaches its maximum counterclockwise excursion, the vortex has fallen apart and moved off the right edge of the bridge.

Vortices form in the wake of an oscillating body from two sources. The von Karman vortex street forms at a frequency determined by the geometry of the bridge and the wind velocity. These vortices form independently of the motion and are not responsible for the catastrophic oscillations of the Tacoma Narrows Bridge. Vortices are also produced as a result of the body's motion. In most cases, the frequency of the vortex formation matches the frequency of the oscillation. The behavior of these vortices depends on the geometry

and the motion of the body. The nature of these motion-induced vortices played a central role in the collapse of the bridge.

Kubo *et al.*⁹ were the first to observe the detailed structure of the wake that forms around the bridge's H-shaped cross section and for a rectangular cross section (which is also prone to violent torsional oscillations). In both cases a regular pattern of vortices appeared on both the upper and lower sides of the bridge deck. They speculated that the spacing between consecutive vortices was the likely cause of different vertical and torsional modes of oscillation observed during the brief lifetime of the Tacoma Narrows Bridge.

Larsen¹⁰ produced the first physical model of the bridge collapse based on the observations in Ref. 9 and his computer simulations. Let us briefly describe his model. We assume that the bridge is oscillating at its resonant frequency with some amplitude. A vortex is formed at the leading edge of the deck on the side in the direction of motion as the angle crosses zero (see Fig. 3 in Ref. 10). The vortex formed suddenly at the front edge of the bridge just as the bridge passed the horizontal position on the shadowed side of the deck. Because a vortex is a low-pressure region (needed to cause the air to circulate around the vortex), a force in the direction of the vortex is produced on the bridge. Each time the bridge is level, another vortex is generated. Once the vortex forms, it will drift down the deck of the bridge producing a time-dependent torque. Larsen made two assumptions based on his observations at dimensionless wind speeds near $UP/D = 4$, where U is the wind velocity, P is the period of oscillation of the bridge, and D is the width of the bridge (our notation is meant to match Larsen's as much as possible). For the Tacoma Narrows bridge, $P = 5$ s and $D = 39'$. He assumed that the vortex drifts at a constant speed of roughly $0.25 U$ and the force on the bridge produced by the vortex is independent of time.

Larsen analyzed this model by considering the work generated by vortices as they drift over the bridge. Figure 3 in Ref. 10 shows the three cases he considered. At wind speeds less than the critical wind speed, the vortices do not cross the entire bridge in one period and produce net torques that dampen the oscillation. At the critical wind speed, the vortex crosses the bridge in exactly one period and the total resulting work is zero. At higher wind speeds, the vortex crosses the entire bridge in less than a period, doing work on the bridge. The reason for the net work is that the vortex spends more time on the leading edge while it is rising (hence a force in the direction of motion). During the descent, the vortex crosses halfway and the force is once again in the direction of motion. As a result, the bridge gains energy and the amplitude of oscillation grows. If the drift speed of the vortices is between $U/4$ and $U/3.6$, then the critical wind speed at which the work becomes positive is $U_c P/D = 3.6 - 4.0$, consistent with measurements. Thus the critical wind speed has been predicted by using only a simple model of vortex motion. Kubo *et al.*⁹ showed that this same pattern could be observed at lower wind speeds and may explain the other observed modes of oscillation. Further simulations by Larsen¹⁰ show that the critical wind speed is increased if the vortex formation at the leading edge is suppressed by replacing the solid trusses with perforated ones.

Despite this success, Larsen's analysis is somewhat incomplete given the available data. In particular, it does not address the dependence of the damping on the wind speed. In

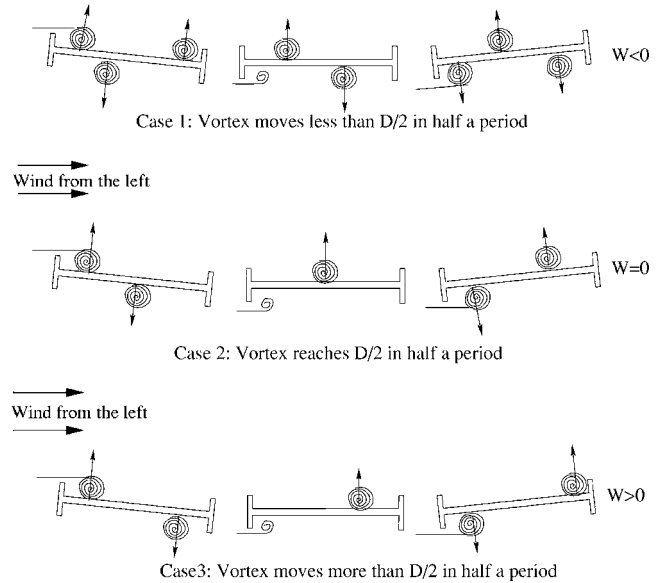


Fig. 4. Larsen's model and analysis of the feedback mechanism. The work can be calculated from the time integral of the force times the velocity of the deck at the point of the force. When the vortex drifts across the deck in exactly one period, the force it produces does no work on the bridge. This condition gives the critical wind speed. Above this wind speed the work is positive. At slightly slower wind speeds, the work is negative. For a drift speed of $U/4$, $U_c P/D = 4$.

dimensionless units the drift time of the vortex across the deck is $t_d = 3.6 - 4.0$. The motion of the bridge is described by

$$\alpha = A \sin \frac{2\pi t}{P}, \quad (4)$$

$$\dot{\alpha} = \frac{A2\pi}{P} \cos \frac{2\pi t}{P}, \quad (5)$$

where α is the angle of the bridge and A is the amplitude of the oscillation. We can also write the torque as

$$\tau = \frac{FD}{2} \left(1 - \frac{2t}{t_d} \right) = \frac{FD}{2} (1 - t/t_d), \quad (6)$$

where F is the force generated by the vortex; Eq. (6) follows from considering the position of the vortex as a function of time. If we take the scalar product of $\dot{\alpha}$ and the torque, $\int_{t=0}^{t_d} \dot{\alpha} \tau dt$, we obtain the work (Fig. 4)

$$\int_0^{t_d} (\tau \dot{\alpha}) dt = - = \frac{FD}{2} A \left[\sin \left(\frac{2\pi}{u} \right) + \frac{u}{\pi} \left(\cos \left(\frac{2\pi}{u} \right) - 1 \right) \right], \quad (7)$$

where $u = U/U_c$. Based on Bernoulli's equation, we assume that F is proportional to U^2 . The resulting dependence of the energy fed into the motion of the bridge by a vortex is shown in Fig. 5 as a function of u . This behavior clearly does not fit the behavior of the bridge at high wind speeds.

The work of Larsen¹⁰ and Kubo *et al.*⁹ suggests that a point vortex model may be reasonably accurate at low wind speeds. However, a number of questions remain. How do the vortices form and how do they drift? If they move at $1/4U$, why? Is the force constant as a function of time? Can we adjust this model to reproduce the wind speed dependence of the damping?

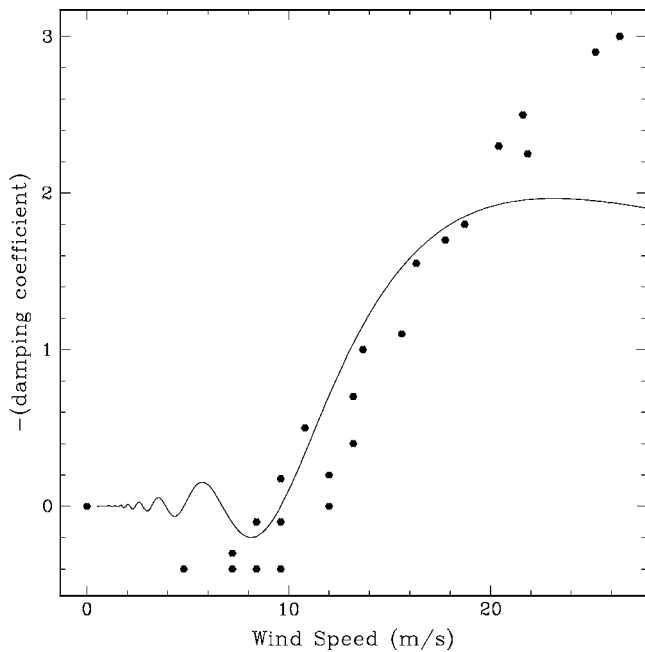


Fig. 5. Additional analysis of Larsen's model compared to wind tunnel data taken from Ref. 3. The work done over one period is the same as the negative damping coefficient. Although the model agrees with the data around the critical wind speed, problems occur at higher wind speeds.

IV. POTENTIAL FLOW MODELS

We will examine several potential flows in order to address these questions. First, we will look at how vortices drift near boundaries. Then we will consider how a vortex drifts near the trailing edge of the bridge. Finally, we will examine the production of vortices at the leading edge.

Potential flows are solutions to the vector Laplace equation. As such, the uniqueness of the solutions allows us to use the method of images. For example, a vortex at a solid boundary (no flow through conditions) can be solved using a vortex of the opposite orientation reflected across the bound-

ary. This same model will apply when the vortex is placed in a uniform flow with a boundary. A two-dimensional vortex is described by $v = \gamma / (2\pi r)$, where γ is the vortex strength. The vorticity transport equation in two-dimensional incompressible flow has the form¹¹

$$\frac{\partial \boldsymbol{\omega}}{\partial t} + (\mathbf{u} \cdot \nabla) \boldsymbol{\omega} = \nu \nabla^2 \boldsymbol{\omega}, \quad (8)$$

where $\boldsymbol{\omega} = \nabla \times \mathbf{u}$ is the vorticity and ν is the viscosity. Because ν is small, the vortex will drift at the speed of the fluid at its center (ignoring its own contribution to the flow). In this case the vortex will drift at

$$v_d = U - \frac{\gamma}{4\pi a}, \quad (9)$$

where a is the distance from the boundary to the center of the vortex. We expect a vortex on the bridge deck to drift at a reduced speed under an external flow.

When the vortex reaches the back edge of the bridge, the local fluid flow may not be along the bridge deck as we have assumed. A laminar-like flow over the back edge must separate from the bridge in order to get over the back truss. This flow will cause the vortex to move off the bridge deck. This separation will reduce the force generated by the vortex at the surface. As a result, the force at the back edge of the deck should be lower than elsewhere on the bridge. Also, as the vortex and the separation line leave the back edge, the reduced pressure within the vortex will pull in fluid from the lower side of the deck, often producing a counter flow vortex beneath the detaching original vortex.

The formation of the vortices is intuitive and provides insight into the large wind speed problems seen in the Larsen model (Fig. 5). First let us consider what happens in the case where the bridge does not move at the onset of an external flow. The fluid will first flow around the solid truss at the leading edge, separating from the boundary (see Fig. 6). Due to the reduced density, a low-pressure region will form behind the truss that will force the gas downward (the divergence-less velocity condition will have the same effect

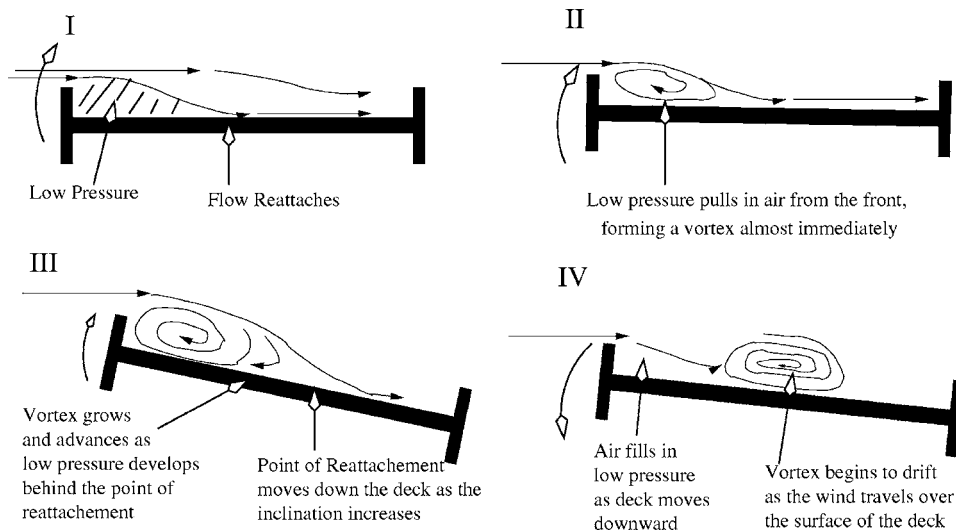


Fig. 6. Vortices are formed in the low-pressure wake of the front edge of the bridge deck. As the bridge deck rises, the point where the flow reattaches moves down the deck. The low pressure region that forms behind this point causes the vortex to grow and move. When the deck begins to move downward, air begins to fill in this low pressure region. This wind will also cause the vortex to drift off the deck at a speed related to the angle of the bridge.

in the incompressible case). Eventually, gas will be pulled backward into this low pressure region producing a vortex. When the bridge is not moving, the vortices remain fixed behind the truss. Furthermore, equal strength vortices form on either side of the deck. Therefore, the drifting of the vortices is a result of the motion of the deck. As the front edge of the deck moves upward, the size of the low-pressure region increases on the top of the deck. During the upward part of the motion, the point on the deck where the flow reattaches to the deck will move down the deck, producing a large low-pressure region from the truss to this point. Once the deck begins moving back down, the vortex will find itself exposed to the steady flow of the wind. This wind will push the vorticity off the back edge. The speed at which the vortex moves will depend on the angle. For large wind speeds, all vortices will be pushed off the back edge by $3/4$ of a period as the entire deck is exposed to the steady wind.

The under side of the bridge is affected in the opposite way while the front edge is moving upward. As the deck moves, the point of reattachment moves toward the front truss, thus filling in the region where the vortex would otherwise form. At best a very small vortex will form. As a result of the motion, a large vortex forms on one side and a small vortex forms on the opposite side. This behavior will repeat every half period of the bridge's motion.

After considering these different aspects of the vortex formation and motion, we have developed a model, which also depends crucially on vortex formation and drifting. Our model differs from Larsen's. First, the vortex motion across the bridge deck will not be uniform. In the first quarter of the period (as the leading edge rises from level), the vortex grows due to the movement of the point of reattachment back along the deck. Because the vortex begins at the front truss, the torque will have the same sign as the angular velocity for the first quarter period until the maximum height it reached. The exact behavior of the torque will depend on the wind speed. When the bridge reverses its direction of motion (leading edge falls), the vortex begins to drift down the bridge. The local wind velocity will govern the drift speed. This speed will depend on the angle of the bridge and the strength and position of the vortex. We will use the $U/4$ constant wind speed in our models for simplicity. This choice should be thought of as a leading order approximation based on observations from simulations, rather than a derivable result (see Ref. 10 and our results in our simulations discussed in the following). Finally, the torque generated by the vortex will decrease as it moves off the back edge of the bridge. The net result is that the torque is large at the beginning of the oscillation when the angular velocity is high and the magnitude of the torque is smaller later in the motion when it is out of phase with the angular velocity of the bridge.

At very high wind velocities, the size of the vortex grows to the size of the bridge deck and its behavior can again be simply described. As the bridge moves, it creates a low pressure region that grows to cover the entire deck. The pressure in the vortex can be approximated by a step function that moves across the bridge until a uniform low pressure is established across the upper deck. When the wake moves beyond the back edge, flow entering from the opposite side of the bridge fills in the low pressure region on the upper deck, reducing the pressure almost uniformly. As a result, the pressure will decay without large asymmetries along the length of the bridge and the torque will remain approximately zero.

To generate a single model on all scales capable of de-

scribing the data, we combined the above-mentioned vortex formation process into the formation of leading point vortex (identical to that of Larsen)¹⁰ and a trailing step function (as we have described in terms of the high wind speed behavior). This step function is intended to approximate the pressure of the extended vortex into a force at a single point plus some extended low pressure. Linear and quadratic wind speed dependence were used for the force generated by the vortex and step function, respectively. Such a model is based on the separation of the low pressure that generates the vortex and the reduced pressure generated by the vortex itself. These choices will allow us to recover Larsen's model at low wind speeds and the single large vortex at high wind speeds. The constant pressure distribution caused by the separation moves along the deck at the speed of the front edge of the vortex ($U/2$) while the vortex is centered on the region and thus moves at $U/4$. The torque due to the extended low-pressure region behind the truss gives a damping coefficient using

$$\begin{aligned} \int_0^{t_d} (\tau \dot{\alpha}) dt &= A \left[u^2 \int_0^{2D/u} [(D^2 - (tu/2 - D)^2) \dot{\alpha}] dt \right. \\ &\quad \left. + 10u \int_0^{4D/u} [(D - tu/4) \dot{\alpha}] dt \right] \\ &= -\frac{5}{8\pi^2} \left[u^3 \left(24\pi \cos\left(\frac{48\pi}{5u}\right) - 5u \sin\left(\frac{48\pi}{5u}\right) \right) \right. \\ &\quad \left. + 24\pi \right] - \frac{5u}{4\pi} \left[48\pi \sin\left(\frac{96\pi}{5u}\right) \right. \\ &\quad \left. + 5 \cos\left(\frac{96\pi}{5u}\right) - 5u \right], \end{aligned} \quad (10)$$

where D is the width of the deck. This model is also motivated by our observations of the pressure in the numerical calculations described in Sec. V. The first term represents the combined torque from the step function and the second term represents the torque from the point vortex. The relative value of ten between the two terms was chosen by observation of the relative influence of the vortex and step function at different wind speeds.

The results generated by this model are shown in Fig. 7. The asymmetry in the torque generated by the growing phase allows us to recover the asymptotic linear behavior that is seen in wind tunnel data. Furthermore, the critical wind speed is found to be consistent with experimental values. By adjusting the overall amplitude, the model is found to be consistent with the data in Ref. 3.

The small vortex model used by Larsen is a low wind speed approximation to our model. If the wind speed is sufficiently low, the vortex remains on the bridge for at least one period. As a result, the time when the vortex is growing is less significant given the long time of interaction. Furthermore, the differences in drift speed become less significant because the variation occurs on a time scale much shorter than the time that the vortex is on the bridge. Finally, the points of reattachment and separation are much closer to the trusses at low speeds, reducing the effects seen at both ends. The result is that our model and Larsen's give essentially the same results under these conditions. However at speeds in excess of $UP/D=5-6$, the low wind speed approximation does not hold.

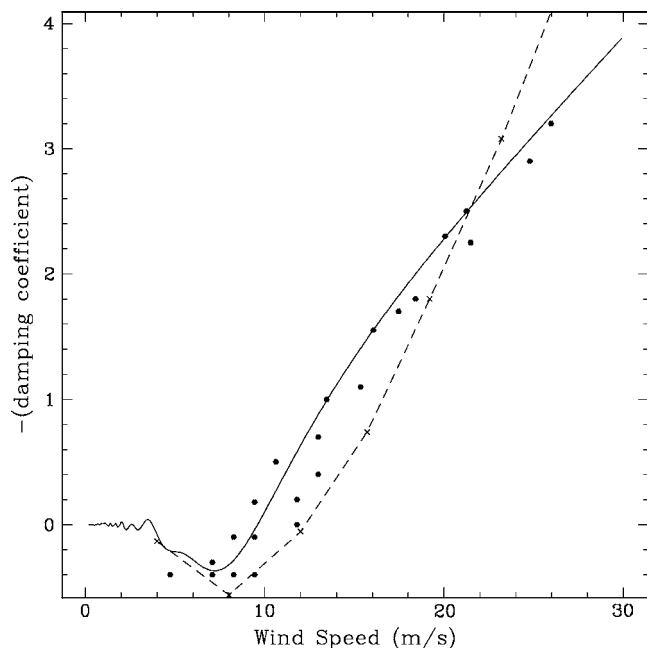


Fig. 7. The results of our model are compared to data taken from wind tunnel tests (points) and simulations using VXF FLOW—Ref. 11 (crosses and dotted line). Our model does not suffer from the large wind speed deviations seen in Larsen’s model (Ref. 10). It also successfully describes the low wind speed behavior. The simulation, which guided the model, is further from the experimental data. The error of the simulated data is likely to be substantial, because we were unable to simulate more than ten periods. The simulated damping coefficients shown are the average over all periods after the first.

V. HISTORICAL AND COMPUTATIONAL EVIDENCE

We have discussed a model based mainly on simplified laminar flows. More rigorous evidence is required to support this model rather than just the fit to the wind speed data. It must be shown that such a flow appears when we calculate the full flow numerically. In particular, we want to show that the high wind velocity flow is different from that observed in Refs. 9 and 10.

The most exciting and useful physical evidence comes from the film coverage of the November 7, 1940 incident. At one point during the oscillation, the roadway appears to break up throwing cement dust into the air. In several frames from the original movie (see Fig. 3), this dust reveals the vortex motion. The cement and dust become caught in a vortex that drifts along the bridge deck at a rate similar to that seen in our simulations. (It is not possible to determine the exact rate relative to the wind velocity because the instantaneous wind velocity is unknown.) This video supports two important points in this argument: the existence of drifting vortices on the deck, and the fact that the vortex crosses the midway point in less than one period, a requirement for negative damping.

The engineers present at the bridge did not risk life and limb to obtain a more complete set of wind and pressure measurements. As a result, this single observation captured on film seems to be the only historical evidence from the bridge itself. We are forced to rely on numerical simulations to fill in the gaps. Our simulations were conducted using VXF FLOW software produced by Guido Morgenthal.¹¹ This code uses discrete vortex methods to determine the flow.

The discrete vortex method is a way of solving the incompressible Navier-Stokes equation in two dimensions. Because all variations along (rather than across) the bridge are slow, we assume that the fluid flow across the bridge is approximated by a two-dimensional flow; that is, if z is the dimension along the bridge, all in the fluid are assumed to be constant in the z direction. We regard the fluid as incompressible because the velocity of sound (a measure of the velocity scale at which the compressibility of the flow becomes important) is of the order of 1000 km/h, while the flow across the bridge is only of order 60 km/h.

The incompressible Navier-Stokes equations are

$$\rho(\vec{v} + \vec{v} \cdot \nabla \vec{v}) = \nabla p - \eta \nabla^2 \vec{v}, \quad (11)$$

$$\nabla \cdot \vec{v} = 0. \quad (12)$$

The vorticity, $\vec{\omega} = \nabla \times \vec{v}$, satisfies

$$\vec{\omega} + \vec{v} \cdot \nabla \omega = -\bar{\eta} \nabla^2 \vec{\omega}. \quad (13)$$

That is, the vorticity is convectively dragged with the fluid, with the specific viscosity acting like a diffusion term. In the discrete vortex technique, instead of modeling the fluid as a continuous velocity field, the flow is divided into a smooth (usually constant) flow plus “particles” or elements of vorticity. These discrete particles of vorticity are convected with the fluid, while it is the vorticity elements themselves that determine the fluid flow. That is, the fluid flow is assumed to be composed of the smooth (usually everywhere constant) background flow, plus contributions from each element of the vorticity. The viscosity is modeled in two ways. One is by assuming that the viscosity acts to expand the size of the vorticity element, making the vortex core larger by a diffusive process, and the other is by perturbing the motion of the vorticity element by a random walk, with the coefficients of the random walk selected so as to give the above-presented equation in the mean for a large number of particles. This random walk component, which is the main way in which the viscosity is modeled, seems to be crucial to obtaining the correct limit for the fluid motion for large numbers of vorticity elements. See Ref. 11 for a detailed discussion of this aspect.

The vorticity is created at the bridge-air interface. The boundary conditions that the velocity be zero at the interface can only be modeled in terms of these vortex elements if this interface constantly creates new vorticity. Thus, small discrete vorticity elements are created at the surface, and then leave the surface due to the random walk component in their motion which models the viscosity. There are numerous subtleties in the development of a discrete vortex code, and we refer the reader to Ref. 11 for a further explanation.

The more common finite element techniques represent the flow by defining the velocity field within a set number of finite volumes that tessellate the space. Because of the finite grid size separating the volume elements, the equations of motion of the fluid are not satisfied on scales approaching the size of the elements. The resultant discretization errors act as random diffusive force on the fluid and introduce what can be regarded as an effective viscosity. The numerical viscosity inherent in finite element techniques is typically many orders of magnitude larger than the actual viscosity of the air, unless the size of the elements is taken to be so small that the numerical solution becomes prohibitively slow.

The advantage of a vortex model compared to finite element methods is that it solves for the vortex transport explicitly. Because the Reynolds number of the flow across the bridge was so high (of order 10^6), a high numerical viscosity could seriously change the physics of the modeled flow. Vortex methods offer the advantage of removing such grid viscosity, but suffer from relatively poor convergence for smooth flows converging at a rate that goes as $N^{-1/2}$, where N is the number of vortices. However, the ability of present-day computers to handle large numbers (our simulations typically have more than 10^5 vortices in play at any one time), and its ability to model the high Reynolds numbers typical of the bridge without the introduction of artificial viscosity makes using discrete vortex methods the preferred procedure.

In our simulations the deck was constrained to oscillate at a given frequency and amplitude and the resulting fluid flow and pressures along the surface were calculated. These simulations covered a large range of incident wind speeds and amplitudes of oscillation. At each time step, the location and velocity of every vortex was determined along with the pressure along the surface of the bridge. The lift, drag, and the torque were calculated from the pressure along the deck. Because the discrete vortex elements drift at the local wind speed, the vortices are tracers of the velocity field and can also be used to visualize the fluid flow.

At wind speeds below 10 m/s, the simulated pressure and fluid flow are very similar to those described by Larsen.¹⁰ In particular, a vortex is generated at the front and drifts along the deck. This vortex makes the largest contribution to the pressure. When the vortex is created, a more extended low pressure region is created behind the truss as the bridge rises. As the vortex begins to drift, the extended constant pressure slowly disappears leaving only the vortex.

At wind speeds of around 19 m/s, a speed that was observed on the fateful day, turbulence begins to play a more significant role in determining the pressure. As the deck rises, the extended pressure covers over half of the bridge deck. A large vortex forms near the front of the high pressure region. The vortex makes an equal contribution to the extended constant low pressure region behind the truss. As the vortex drifts off the deck, a low pressure covers the deck. This motion varies with the angle of the bridge and is not constant. The flow is turbulent as smaller vortices are shed behind the first. The pressure remains low until the deck is exposed entirely to the wind at $3/4$ of a period when the angle is maximum in the opposite direction. The similarity between the simulation and the original film can be seen in Fig. 8 where a frame from the simulation is shown at the same point in the oscillation cycle as the video frame in Fig. 3.

At wind speeds above 30 m/s, turbulence dominates the flow. As the deck rises, the low pressure moves across the deck, covering it entirely before the deck reverses direction. A single vortex is formed at the front of this region, similar to the slower wind speeds, except it contributes a small force relative to the extended low pressure region. Unlike the slower wind speeds, the vortex behind the front truss is not the only large vortex that forms. Vortices are formed off the front edge at a high frequency and drift at varying speeds. At times these vortices can catch up with the front vortex. Large counter vortices are formed at the back edge as air is pulled from the far side of the bridge to fill in the low pressure. These large vortices influence each other due to the lower or higher pressure regions that form between them. These inter-

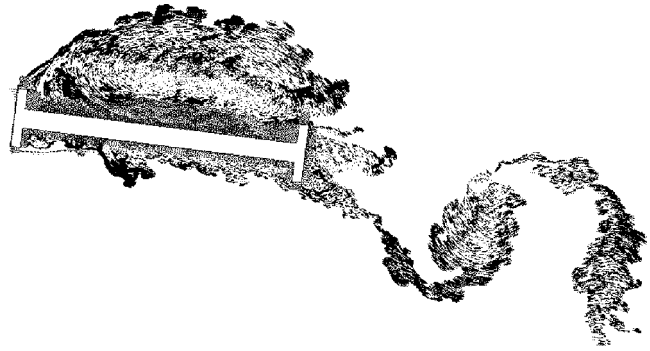


Fig. 8. Frame from the simulation at 19 m/s. There is a large vortex greater than halfway across the bridge as it becomes level. This image is very similar to the frame from the original movie. There is also a low pressure region that covers the length of the deck, which is consistent with our model.

actions will produce unpredictable fluid behavior. Such a highly turbulent flow introduces rapid noticeable changes in the pressure making torque and work calculations highly variable from one cycle to the next. Because the vortices are shed at a high frequency relative to that of the bridge, the contribution of the noise to the work over many periods will be negligible.

The torque calculations were used to generate effective damping coefficients over a range of wind speeds (see Fig. 7). For wind speeds from 4 to 30 m/s, the damping coefficients at 0.3 rad are similar to those measured in Ref. 3. At wind speeds greater than 30 m/s, the negative damping coefficient begins to drop in magnitude. Particularly at high wind speeds, the work is very sensitive to the magnitude of the time step of the discrete code and the period over which the work is averaged. Morgenthal noticed this problem as well.¹¹ His simulations of another bridge section gave a drop in the magnitude of the damping coefficient that was inconsistent with the measurements. Therefore, it is not clear whether the drop in the negative damping at high velocities is a real or computational effect. Because of the noise in the data, the few periods we were able to simulate, and the variability in the simulation output due to the variations caused by the turbulent nature of the flow, the error could be as high as 30%–50% for some points. Furthermore, the experimental data were taken when the bridge was allowed to oscillate freely, with increasing amplitude, while in the simulation the amplitude of the bridge oscillation was fixed.

Given these observations, how does our model discussed in Sec. IV compare to the computational and historical evidence? The generic description of the physics is consistent with the behavior of the bridge over one period of oscillation of the bridge (ignoring the high frequency noise). The vortex forms in a large low pressure region and separates from the front truss as the front deck moves downward. A simplification of this behavior occurs at very high wind speeds when the low pressure covers the entire bridge before the front edge begins to drop. Furthermore, the pressure generated by the vortex seems to decay at the far edge of the bridge. The advantages of this model can be seen in Figs. 9–11. The Larsen model does not adequately explain the data or the simulations at wind speeds above 20 m/s. The fluid flow in Figs. 9–11 is in reasonable agreement with our model.

However, our model is not completely consistent with the general behavior of the bridge. There is no simple math-

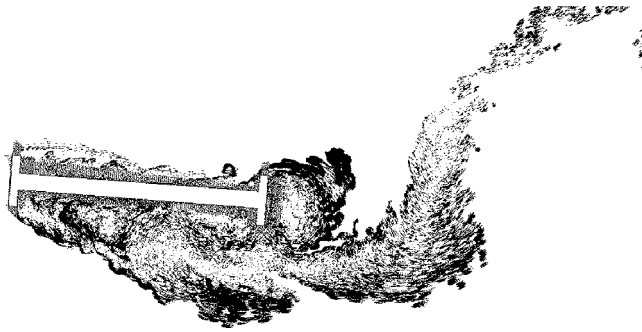


Fig. 9. The simulated flow over the bridge cross section as the deck rises at a wind of 23 m/s. Each point represents a point vortex. (Top Side) A vortex begins to form behind the front edge as a low pressure region forms. This low pressure is due to the separation of the moving fluid from the boundary of the deck. As the deck rises this region will become larger. (Under Side) The vortex that formed on the bottom is being blown off the deck. The pressure on the bottom is decreasing uniformly.

emational description of the torque generated by the windflow that summarizes the pressure and vorticity over the full range of wind speeds. The parameters of the model [given in Eq. (10)] were chosen to be consistent with a large low pressure region at high wind speeds and a single vortex at low wind speeds. Our model suffers some difficulties at intermediate wind speeds, around 10–14 m/s in particular. The constant low pressure region associated with the moving front of the wake does not cover the entire bridge behind the front. Nonetheless, the model uses a step function from the front of the vortex to the windward edge of the bridge to model the behavior of the large vortex. In addition, the velocity of the vortices is taken to be at constant, which is not a good approximation at these speeds, thus only encapsulating the time average behavior.

Further modifications of our model have not been made because they would require more parameters (there are already four parameters in the model). Because our model fits the damping coefficient, such refinements would make little difference in comparison to the data and would only alter the details of the pressure distribution as a function of time. Therefore, given the current data, it would be difficult to improve the model in a measurable way. We have so far assumed that the amplitude dependence of the force is linear (a requirement for the torque to be proportional to $\dot{\alpha}$). This

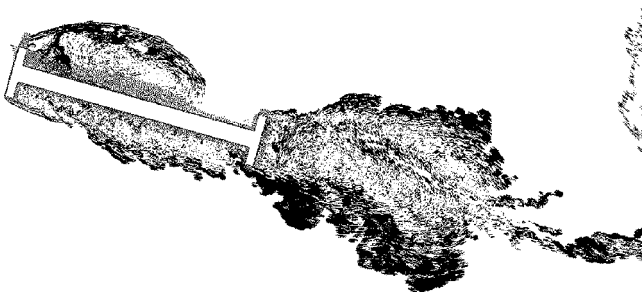


Fig. 10. The simulated flow over the bridge cross section halfway through the rise of the front edge at a wind of 23 m/s. Each point represents a point vortex. (Top Side) The vortex has grown to cover one-half of the deck. Because the deck is still rising, the low pressure region extends from the front of the deck to the backmost edge of the vortex. (Under Side) The bottom of the deck has now been completely exposed to laminar flow. Few vortices remain.

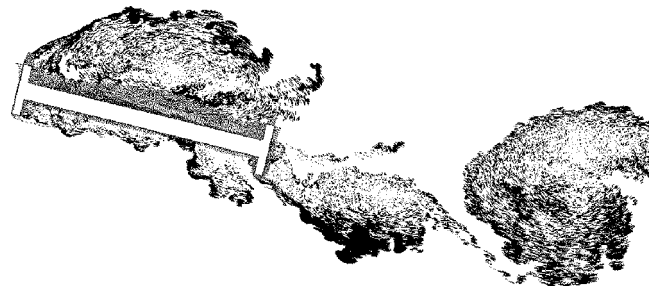


Fig. 11. The simulated flow over the bridge cross section after the full rise of the front edge at a wind of 23 m/s. (Top Side) As the deck descends from the maximum height, the vortex is now being pushed off the back edge. The vortex has grown to cover a large part of the bridge. (Under Side) Laminar flow dominates because the bottom has been completely exposed to the wind.

assumption was tested using torque measurements over a range of amplitudes at a fixed wind speed. The work done in a period generally increases with amplitude. Over a range of amplitudes (that is, the maximum deflection of the bridge) from 0.1 to 0.25 rad the linear assumption appears to be valid. At lower wind speeds the dependence is not certain due to noise caused by turbulence. This problem is most significant at low amplitudes where the fluctuations in the torque from turbulence (random noise) become larger than the average induced torque. Because of the limited time of our simulation, determining the average is difficult.

VI. CONCLUSION

Our goal has been to explain a wide class of observed phenomena by a single simple mechanism. In trying to understand fluid structure interactions such as occurred with the Tacoma Narrows Bridge, accomplishing this goal is non-trivial. Fluid mechanics has typically been the domain of experimentalists because the governing equations are notoriously difficult to solve. Only now is computer power becoming equal to the task. Many past attempts to explain instabilities have been rejected on the basis that they have either gotten the physics wrong or have neglected crucial aspects of the physics. It was Larsen that identified the crucial role played by vortex generation and motion.

Our model is a further step toward the goal of a comprehensive explanation of the phenomena observed on the morning of November 7, 1940. Most of the data can be adequately explained using the vortex-induced model. Further work is required to explain the onset of the violent oscillatory behavior, but it seems that the main features of the wind structure interaction over a large range of wind speeds can be explained by a vortex formation model. However, the range of wind speeds for which the model is applicable has not been fully established. At extreme high and low wind speeds, computations become less reliable and experiments are difficult. At very low wind speeds, vortices may cease to form and at high wind speeds the structure of the wake may lose all periodicity. Nevertheless, our model seems appropriate over a wide enough range that it should be useful for many applications. In particular, it gives physics teachers a model with which to replace the naive and incorrect resonance model so often used in undergraduate lectures.

ACKNOWLEDGMENTS

We would like to thank G. Morgenthal for his generosity in allowing us to use VXF FLOW, the discrete vortex computer code he developed for his Ph.D. We would also like to thank NSERC for support, both in the form of a research grant to WGU and a summer work grant to DG. WGU would also thank the Canadian Institute for Advanced Research for their support.

^{a)}Electronic mail: drgreen@stanford.edu

^{b)}Electronic mail: unruh@physics.ubc.ca

¹Nevell H. Fletcher and Thomas D. Rossing, *Physics of Musical Instruments* (Springer, New York, 1998), 2nd ed. See especially Chaps. 10, 13, and 16.

²K. Y. Billah and R. H. Scanlan, "Resonance, Tacoma Narrows bridge failure and undergraduate physics textbooks," *Am. J. Phys.* **59**(2), 118–124 (1991).

³O. H. Ammann, T. Von Karman, and G. B. Woodruff, "The failure of the Tacoma Narrows Bridge," Report to the Honorable John M. Carmody, Administrator, Federal Works Agency, Washington, DC, 28 March 1941. This report is difficult to find. The Library of Congress does not have a copy, but apparently the Department of Transportation (<http://dotlibrary.dot.gov/>) has. It is also reprinted in *Bulletin of the Agricultural and Mechanical College of Texas, Texas Engineering Experiment Station, College Station, TX, 4th Series, Vol. 15, No. 1, January*

1, 1944. This issue may be equally difficult to find, although the Library of Congress does have a copy.

⁴See for example, David Newland, "Pedestrian excitation of bridges: Recent examples," in *Proceedings of the Tenth International Conference on Sound and Vibration*, Stockholm, July 2003, http://www2.eng.cam.ac.uk/~den/pedestrian_excitation.pdf.

⁵Th. von Karman, "Über den Mechanismus des Widerstandes, den ein bewegter Körper in einer Flüssigkeit erfährt," *Göttinger Nachrichten Math. Phys. Klasse* **509**, 547 (1911).

⁶P. J. McKenna, "Large torsional oscillations in suspension bridges revisited: Fixing an old approximation," *Am. Math. Monthly* **106**, 1–18 (1999).

⁷P. J. McKenna and Cilliam O'Tuama, "Large torsional oscillations in suspension bridges revisited again: Vertical forcing creates torsional response," *Am. Math. Monthly* **108**, 738–745 (2001).

⁸Barnet Elliott, Harbine Monroe, and Aug. von Boecklin, "The collapse of the Tacoma Narrows Bridge." Film available from The Camera Shop, Tacoma, WA, (www.camerashoptacoma.com/). Frames from the film are used with permission of The Camera Shop.

⁹Y. Kubo, K. Hirata, and K. Mikawa, "Mechanism of aerodynamic vibration of shallow bridge girder section," *J. Wind. Eng. Ind. Aerodyn.* **42**, 1297–1308 (1992).

¹⁰A. Larsen, "Aerodynamics of the Tacoma Narrows Bridge – 60 years later," *Struc. Eng. Intern.* **4**, 243–248 (2000).

¹¹G. Morgenthal, "Aerodynamic analysis of structures using high-resolution vortex particle methods," Ph.D. thesis, Cambridge University, 2002.